3D Imaging of Microstructural Evolution in SOFC Anodes

George J. Nelson
Assistant Professor
Mechanical and Aerospace Engineering
University of Alabama in Huntsville

Overview

- The Solid Oxide Fuel Cell
- Why Three-Dimensional Imaging?
- SOFC Anode Degradation
  - X-ray nanotomography measurements
  - Characterization and analysis of microstructure
  - Identification of degradation mechanisms
- Summary and Conclusions
- Potential Extensions

The Solid Oxide Fuel Cell (SOFC)

- Electrolyte: solid ion conducting ceramic
- Key microstructural features:
  - Porous electrodes
  - Dispersed reaction sites

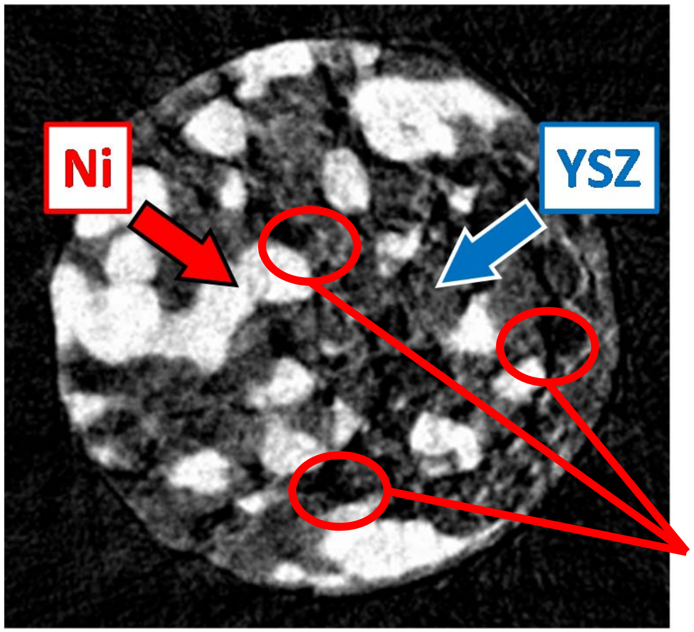

Triple Phase Boundary (TPB)

Planar SOFC

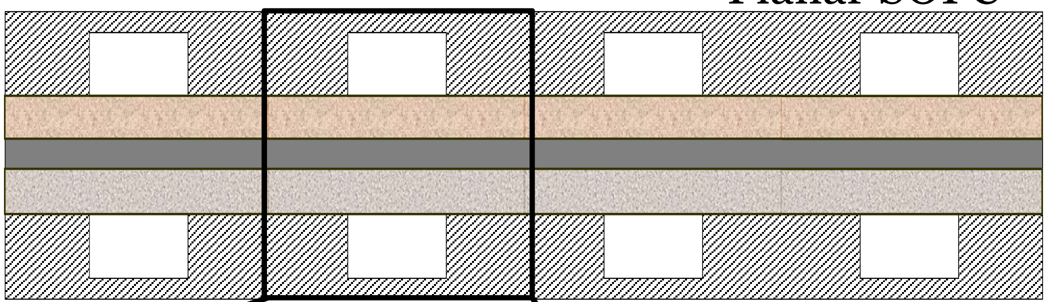

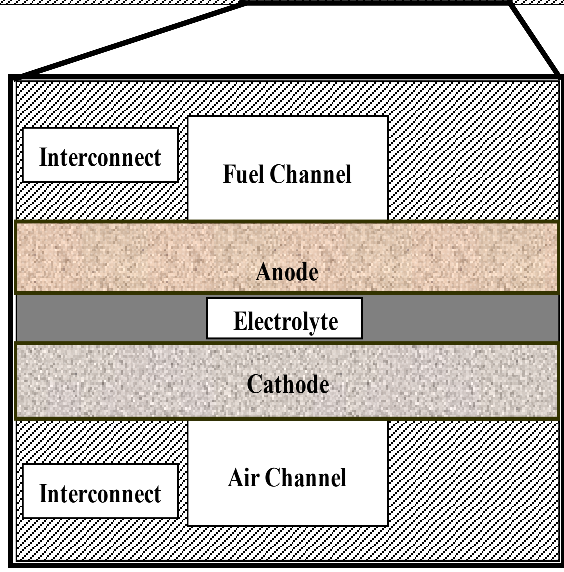

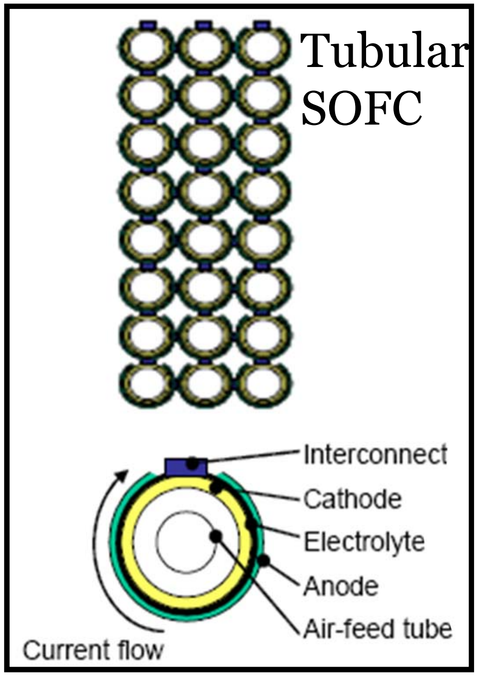

(Fuel Cell Handbook, 2004)

The Need for 3D Image Data

- 3D networks supply reactants to reaction sites.
- 3D microstructure evolves during operation.
- 2D data i

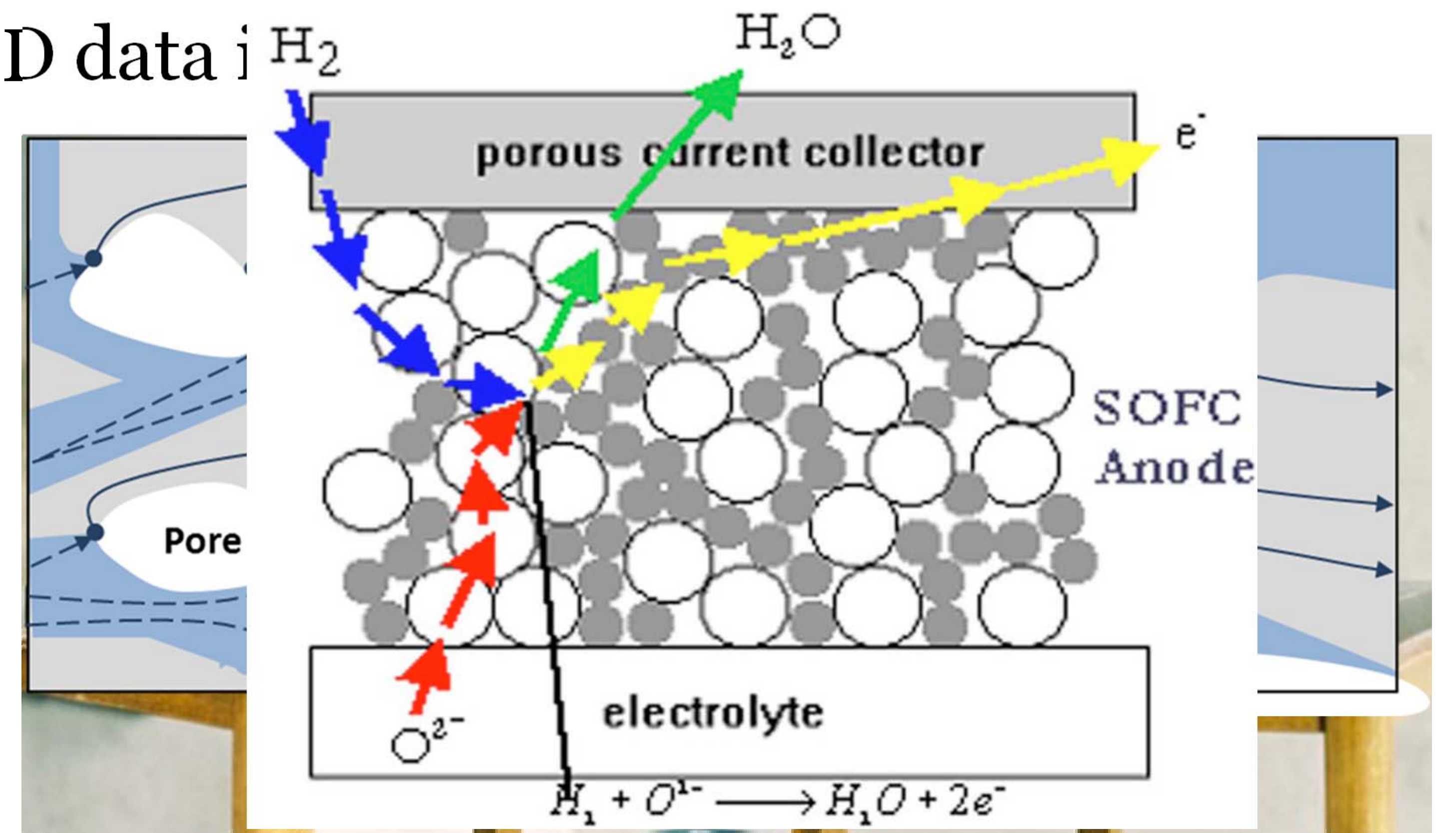

Cannarozzo et al., J. Fuel Cell Sci. Tech., **4**(2) 99-106, 2007.

M. Raetz, *Yes/No*

Observing SOFC Microstructure

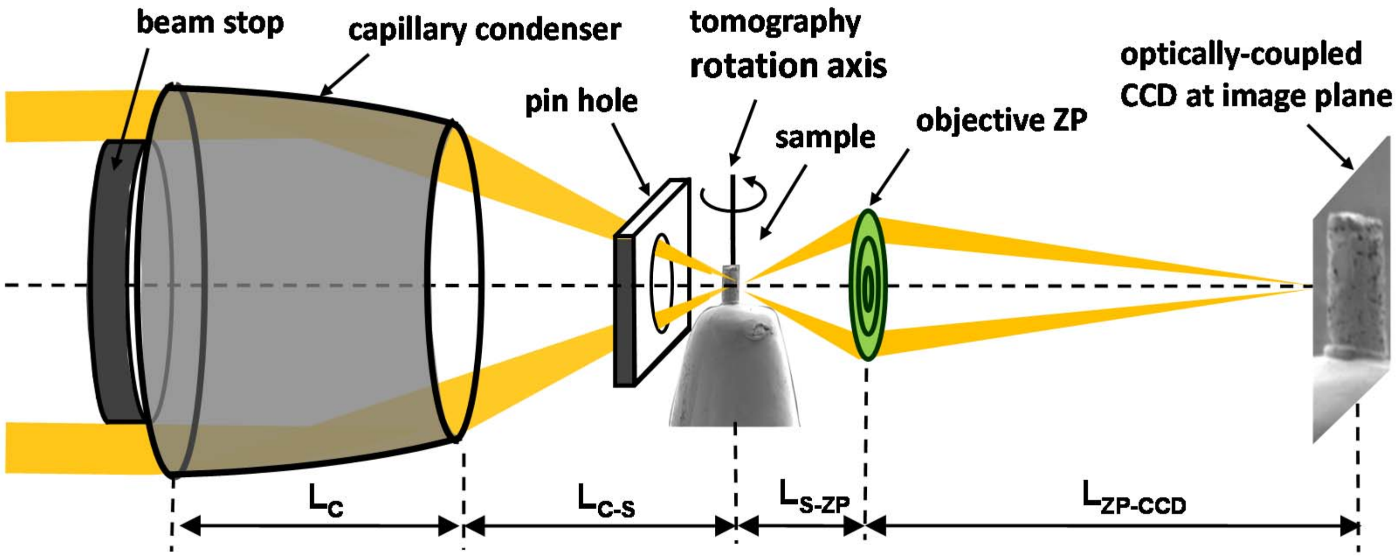

- Transmission x-ray microscope
  - Condenser gathers monochromatic x-ray beam and directs it onto sample.
  - Fresnel zoneplate lens focuses x-rays.
  - CCD records the final x-ray image.
- Absorption contrast imaging
  - X-ray nanotomography performed above and below x-ray absorption edge.

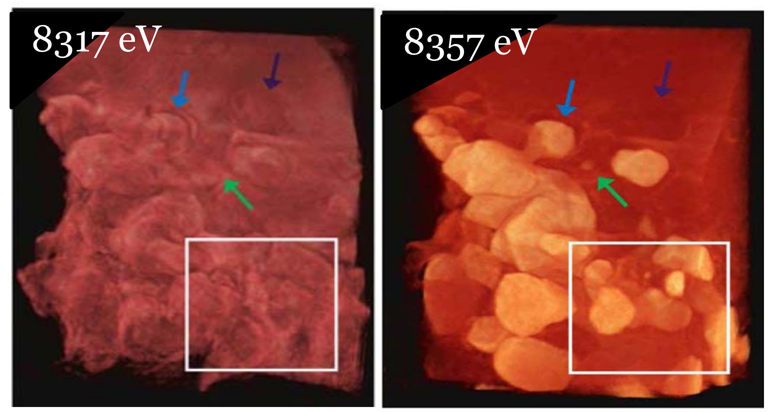

Below Edge　　Above Edge

K. N. Grew, Y. Chu, W. K. S. Chiu et al., *J. Electrochem. Soc.*, **157**(6) B783-BB792 , 2010.

Experimental Details

- Samples taken from cells operated in long term SOFC tests (Faes et al., *Fuel Cells*, **9**(6), 841-851, 2009).
- X-ray absorption contrast imaging applied to map 3D anode microstructure and composition while preserving samples.
- Multiple representative volume elements (RVEs) extracted from sample x-ray nanotomography data.

Breakdown of sample set for stacks based on the fine reference microstructure.

Stack	Operational Time (h)	RVE Replicates per Sample	RVE Replicates per Stack
Reference	0	REFN23 (3), REFN25 (3)	6
Stack A	158	SAC4-C01 (2), SAC4N01 (2), SAC4N11 (2)	6
Stack B	240	SBC1-C01 (2), SBC1N27 (3)	5
Stack C	1130	SCC3-C01 (2), SCC3N12 (2)	4

G. J. Nelson, W. K. S. Chiu et al., Acta Materialia, **60** *3491–3500*, 2012.

Comparison to SEM Results

X-ray Nanotomography

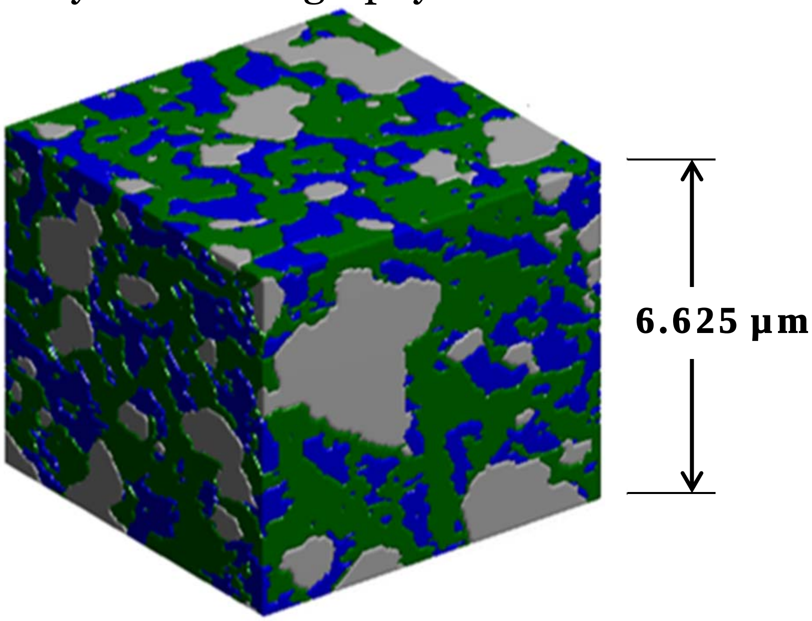

Representative Volume Element (RVE)

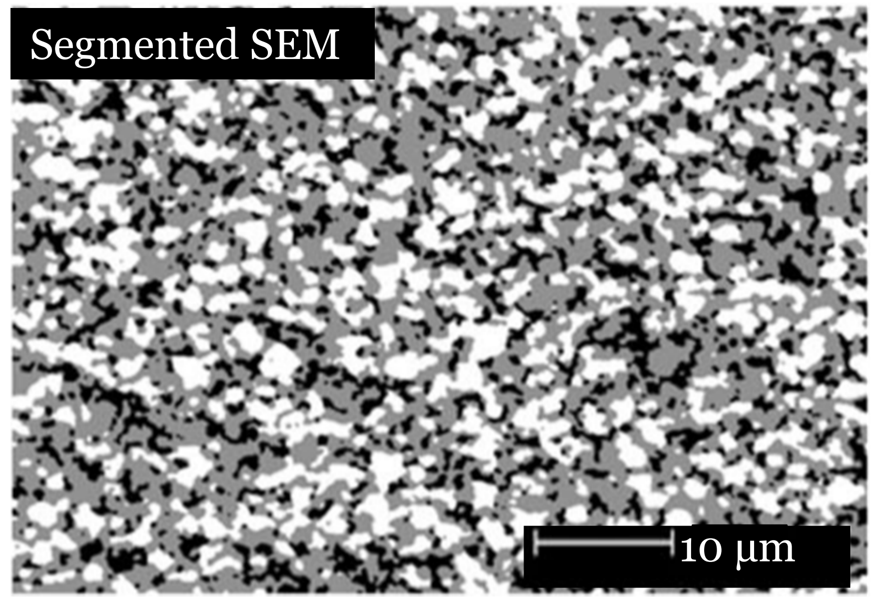

Faes et al., *Fuel Cells*, **9**(6), 841-851 2009

- X-ray nanotomography phase sizes are within experimental error of SEM stereological results.

Stack of Origin (Test Time)	Mean Ni Particle Diameter, µm	
	X-ray Nanotomography	SEM Sectioning
Reference (t = 0 h)	0.66 (± 0.25)	0.58 (± 0.25)
Stack A (t = 158 h)	0.83 (± 0.16)	0.67 (± 0.31)
Stack B (t = 240 h)	0.91 (± 0.13)	0.70 (± 0.33)
Stack C (t = 1130 h)	0.77 (± 0.13)	0.73 (± 0.35)

Anode Microstructural Evolution

- Nanotomography data analyzed for multiple RVEs.
- Distinct growth seen in mean diameter of Ni phase.
  - Large initial growth constrained after longer operation.
- Behavior suggests a pinning mechanism.
  - Ceramic YSZ restricts further growth of Ni.
  - Critical diameters follow YSZ trends.

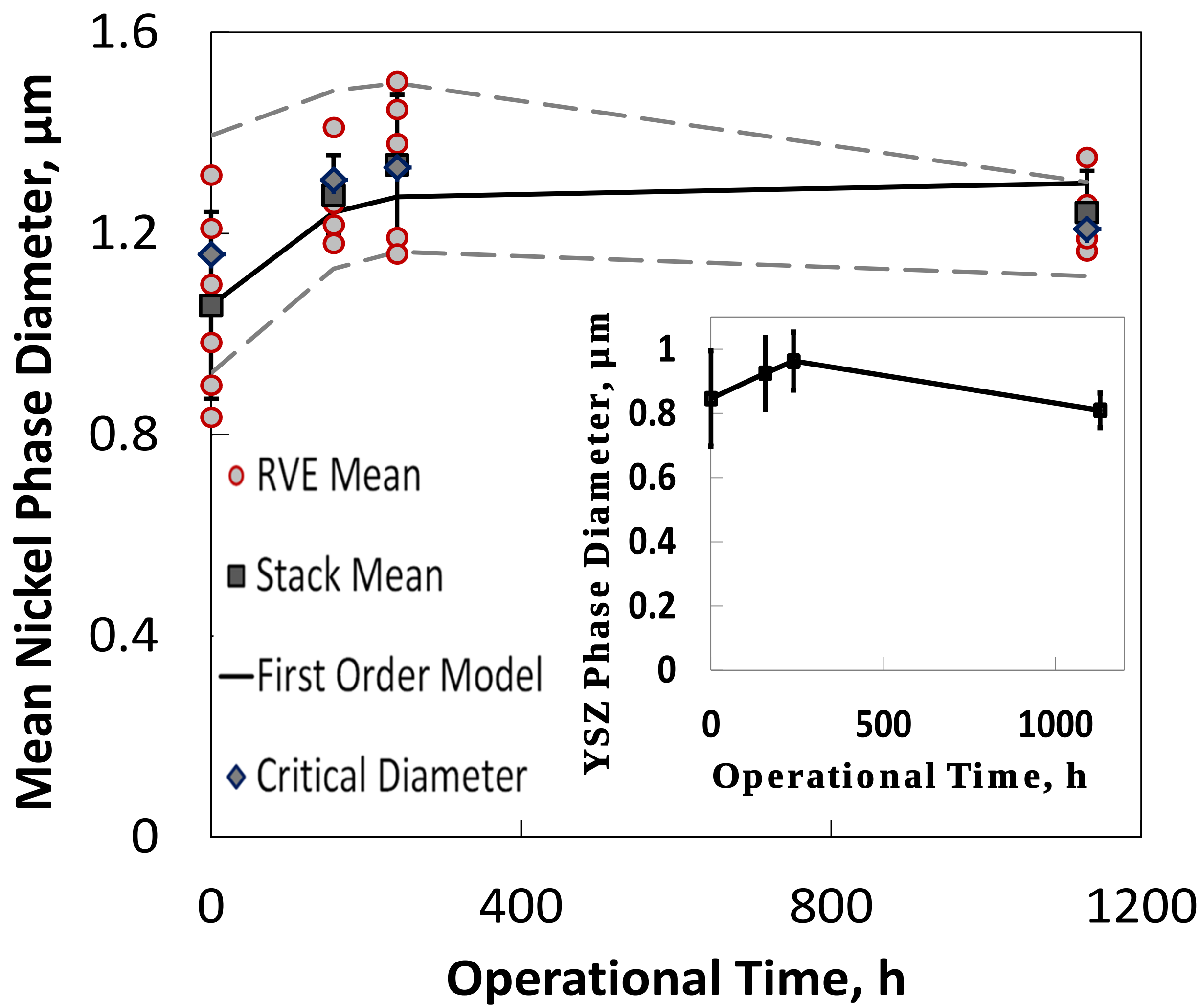

G. J. Nelson, W. K. S. Chiu et al., Acta Materialia, **60** *3491–3500*, 2012.

Impacts of Microstructural Evolution

3D IMAGING REVEALS PHYSICAL MECHANISM & PERFORMANCE IMPACTS.

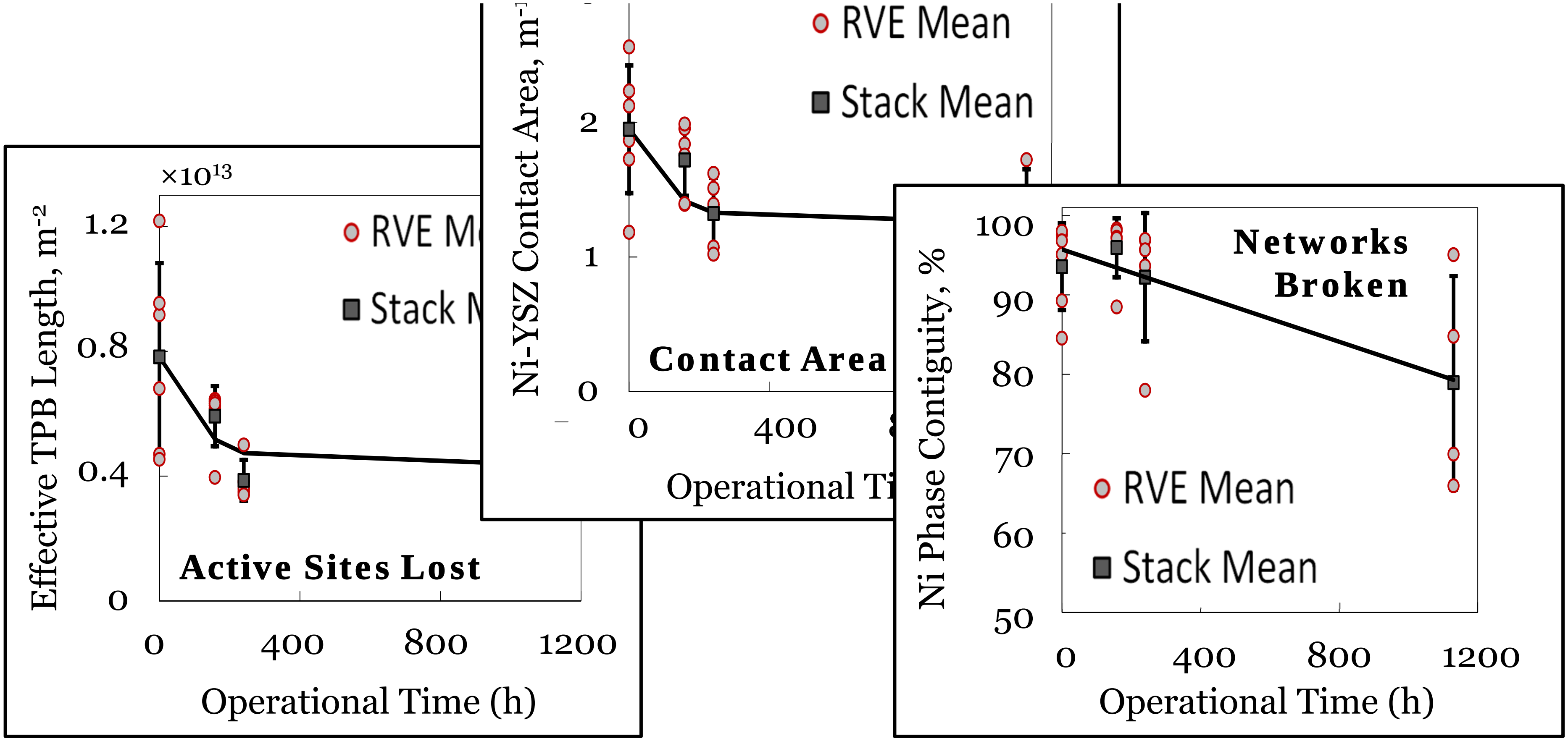

Influence of operational time				
	d_{Ni}	TPBL Nom. (Eff)	Ni-YSZ Contact Area Nom. (Eff.)	Ni Contiguity
p-value	0.0184	0.0066 (0.0133)	0.0084 (0.0186)	0.0198

Summary and Conclusions

- SOFCs and other energy storage and conversion devices:
  - 3D systems of mixed functional materials
  - Require 3D image data for complete analysis
- X-ray nanotomography can provide such data.
- Methods are proven for SOFC anodes
  - 3D data provides insight into Ni coarsening and performance degradation not accessible with 2D data.
    - Coarsening controlled by phase interaction, pinning mechanism.
    - Network breakdown increases active site and conductivity loss.
- Methods are applicable to batteries, solar cells, and other energy storage and conversion devices.

Further Applications

PEM Fuel Cells

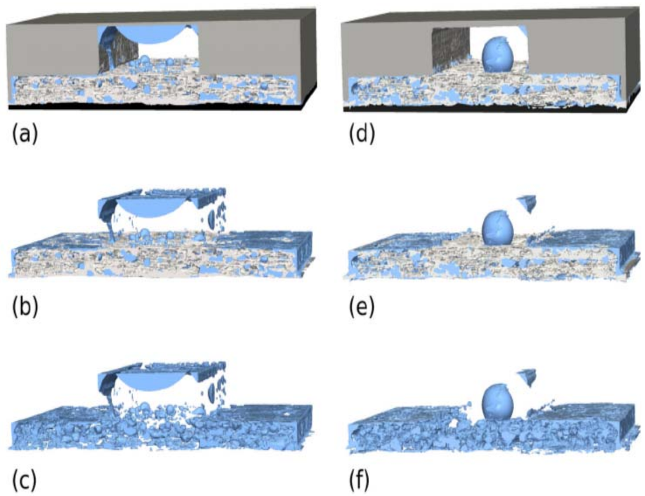

Eller et al., *J. Electrochem. Soc.*, **158**(8) B963-B970, 2011.

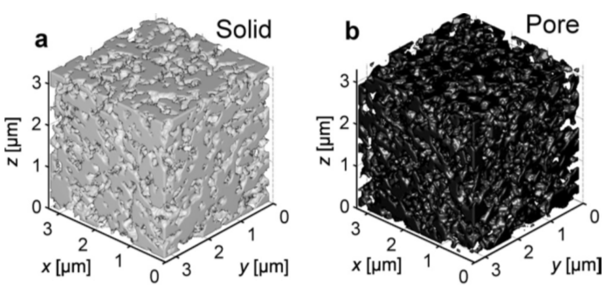

Epting et al., *Adv. Funct. Mater.*, **22** 555-560, 2012.

Batteries

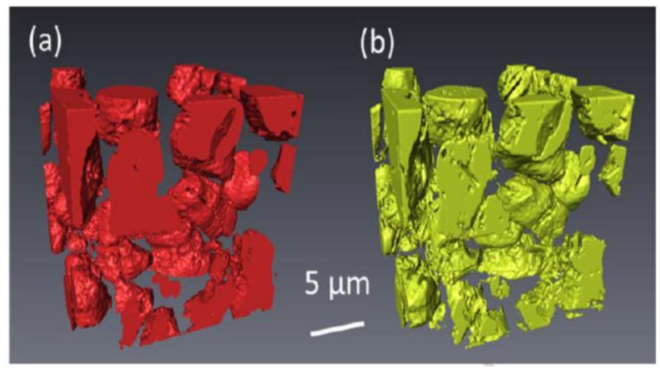

Chen-Wiegart et al., *Electrochem. Comm.*, **21** 58-61, 2012.

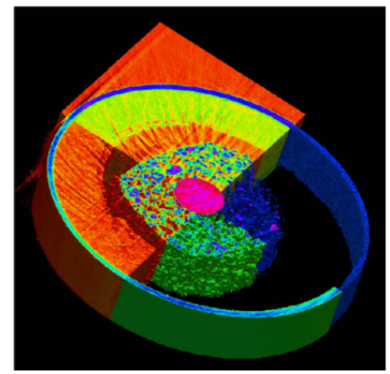

Haibel et al.,*J. Electrochem. Soc.*, **157**(4) A387-A391, 2010.

Ceramic Foams and Catalysts

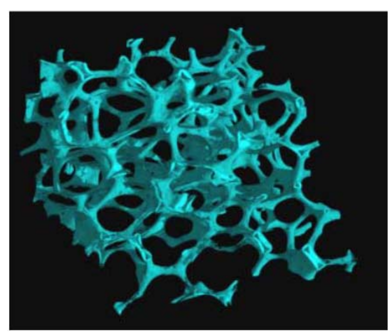

Petrasch et al., *J. Quant. Spectrosc. Radiat. Transfer*, **105** 180–197, 2007.

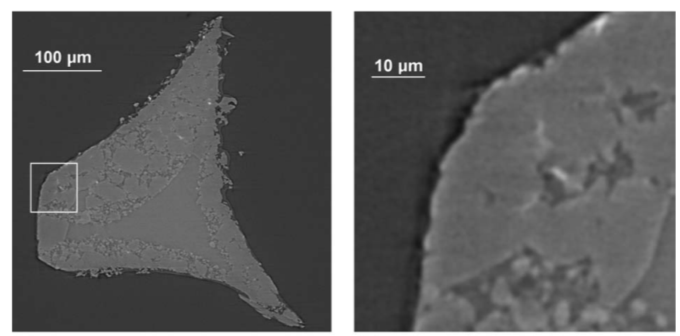

Haussener et al., *J. Heat Transfer*, **132** 023305 , 2009.

Chemical Composition Mapping

- X-ray absorption near edge structure (XANES)
  - Scanning sample over a broader spectrum discerns chemical species.
- Technique also applicable to:
  - Battery electrodes
  - Super capacitors
  - Solar cells

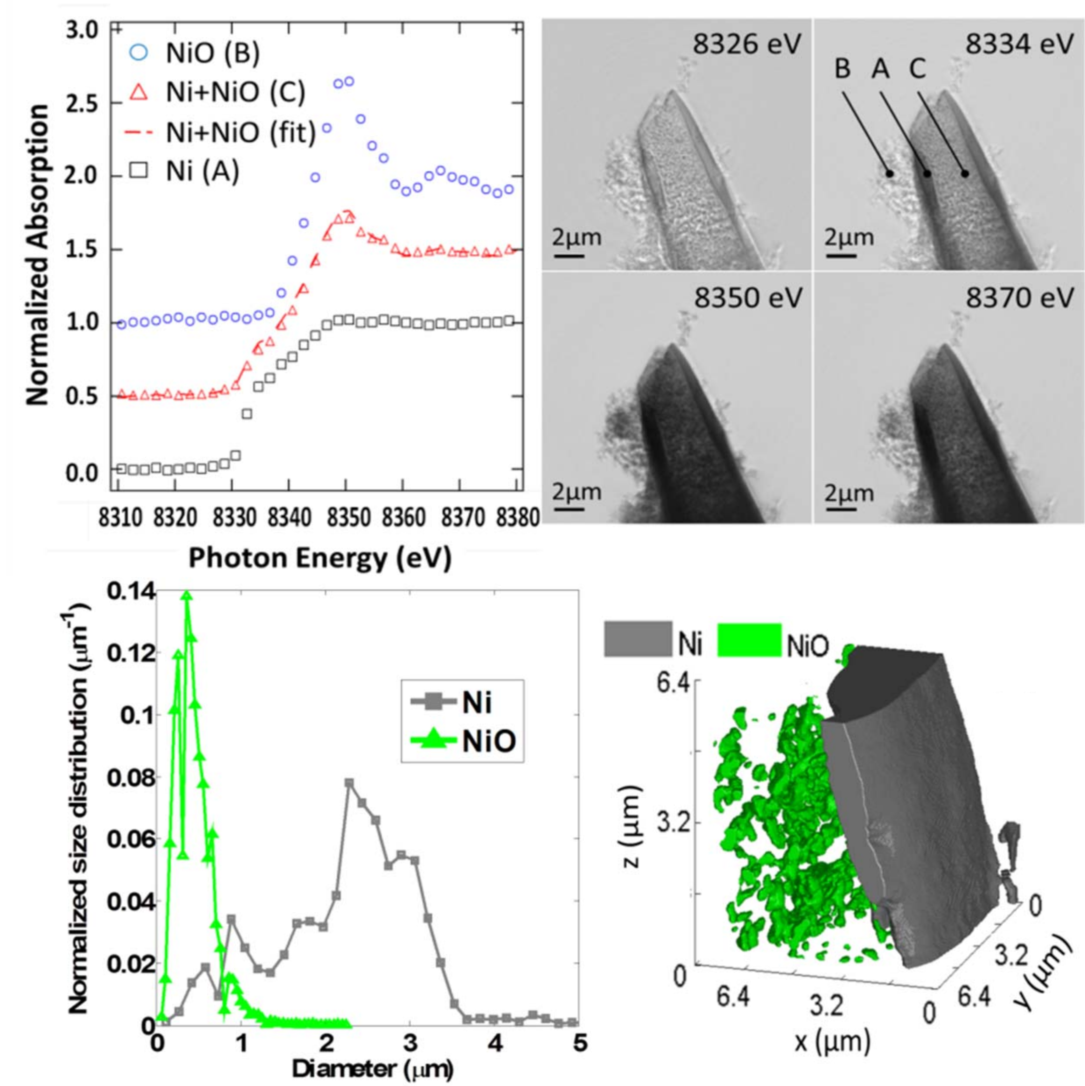

G. J. Nelson, W. K. S. Chiu et al., *Appl. Phys. Lett.*, **98** 173109 , 2011.

Acknowledgements

- Energy Frontier Research Center on Science Based Nano-Structure Design and Synthesis of Heterogeneous Functional Materials for Energy Systems (HeteroFoaM Center) funded by the U.S. Department of Energy, Office of Science, Office of Basic Energy Sciences (Award DE-SC0001061), Prof. Kenneth L. Reifsnider, Director.
- National Science Foundation Award CBET-1134052
- Prof. Wilson K. S. Chiu, University of Connecticut
- Prof. Anil Virkar, University of Utah
- LENI, École Polytechnique Fédérale de Lausanne
- Dr. Kyle Grew, Army Research Laboratory

Supplemental Slides

Electrochemical Storage & Conversion

- Distinct arrangements of materials, phases, structures
- Functionally designed material systems
- Microstructure is critical to performance and reliability.

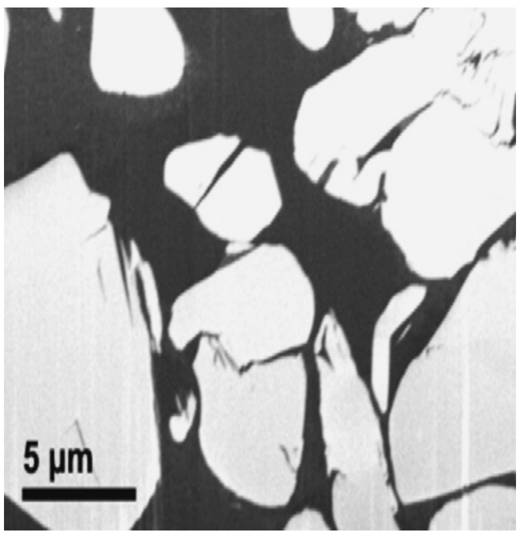

Li-Ion Batteries

J.R. Wilson, S.B. Barnett et al., J. Power Sources, ***196*** *3443–3447*, 2011.

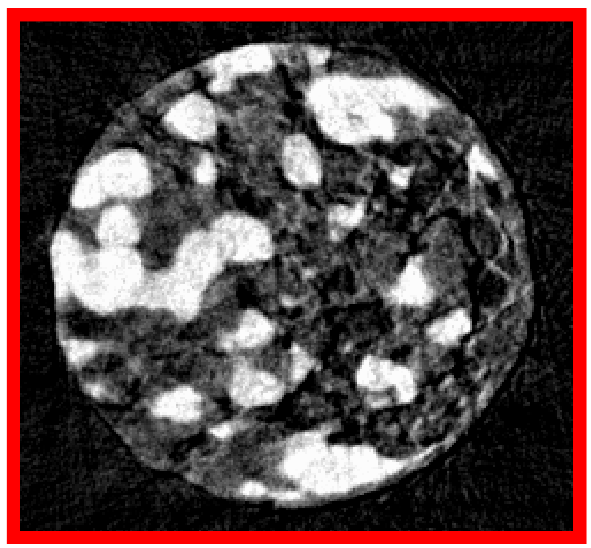

Solid Oxide Fuel Cells

G. J. Nelson, W. K. S. Chiu et al., Acta Materialia, **60** *3491–3500*, 2012.

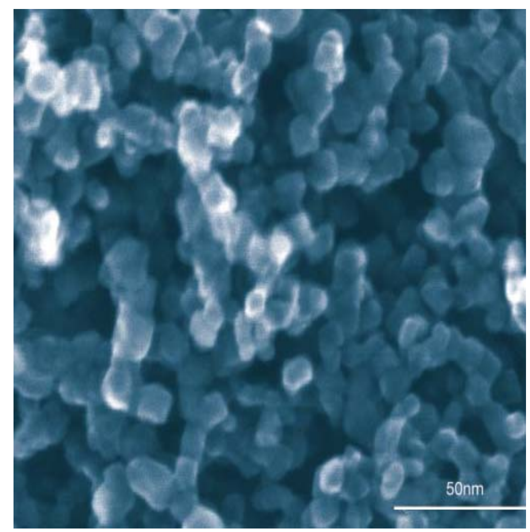

Dye-Sensitized Solar Cells

M. Graetzel, Nature, ***414*** *338-344*, 2001.

Basic Fuel Cell Operation

- Conversion of chemical energy to electrical energy.
  - $H_2 + ½\, O_2 \rightarrow H_2O$
- *Anode:* Oxidation
- *Cathode:* Reduction
- *Electrolyte:* Transfer of ions to complete reaction.

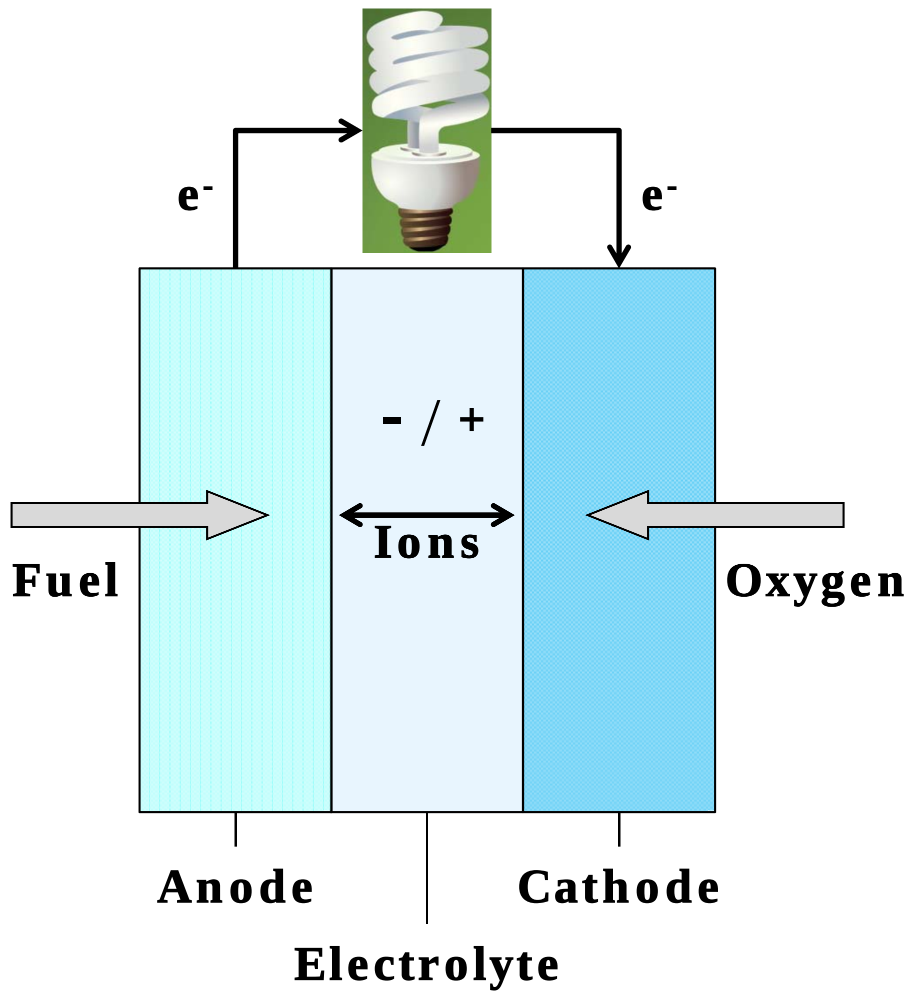

Major Types of Fuel Cells

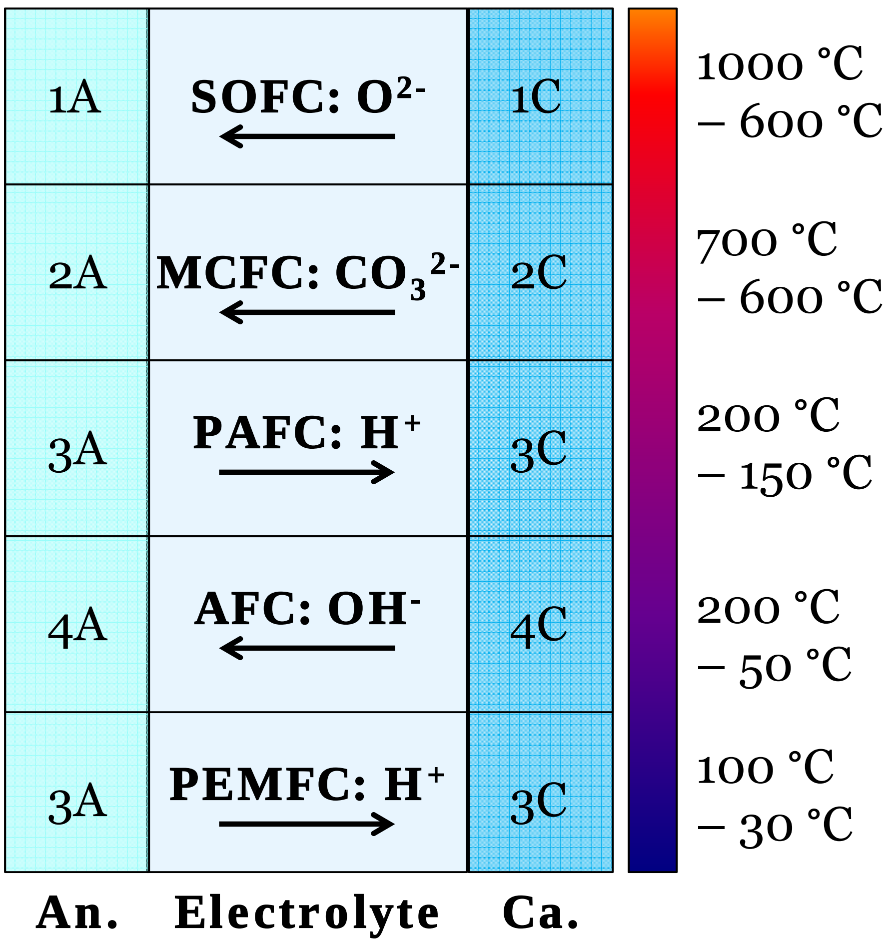

- Classified by electrolyte:
  - Solid Oxide Fuel Cell
  - Molten Carbonate Fuel Cell
  - Phosphoric Acid Fuel Cell
  - Polymer Electrolyte Fuel Cell
  - Alkaline Fuel Cell

	Anode Reaction (A)	Cathode Reaction (C)
1	$H_2 + O^{2-} \rightarrow H_2O + CO_2 + 2e^-$ $CO + O^{2-} \rightarrow CO_2 + 2e^-$	$½O_2 + 2e^- \rightarrow O^{2-}$
2	$H_2 + CO_3^{2-} \rightarrow H_2O + 2e^-$ $CO + CO_3^{2-} \rightarrow 2CO_2 + 2e^-$	$½O_2 + CO_2 + 2e^- \rightarrow CO_3^{2-}$
3	$H_2 \rightarrow 2H^+ + 2e^-$	$½O_2 + 2H^+ + 2e^- \rightarrow H_2O$
4	$H_2 + 2(OH)^- \rightarrow H_2O + 2e^-$	$½O_2 + H_2O + 2e^- \rightarrow 2(OH)^-$

SOFC Anode Degradation

- Electrode microstructural evolution causes substantial power loss.
- Ni coarsening is a widely observed anode degradation mechanism.
- 3D imaging captures microstructural morphology (shape and size) and topology (network connectivity).

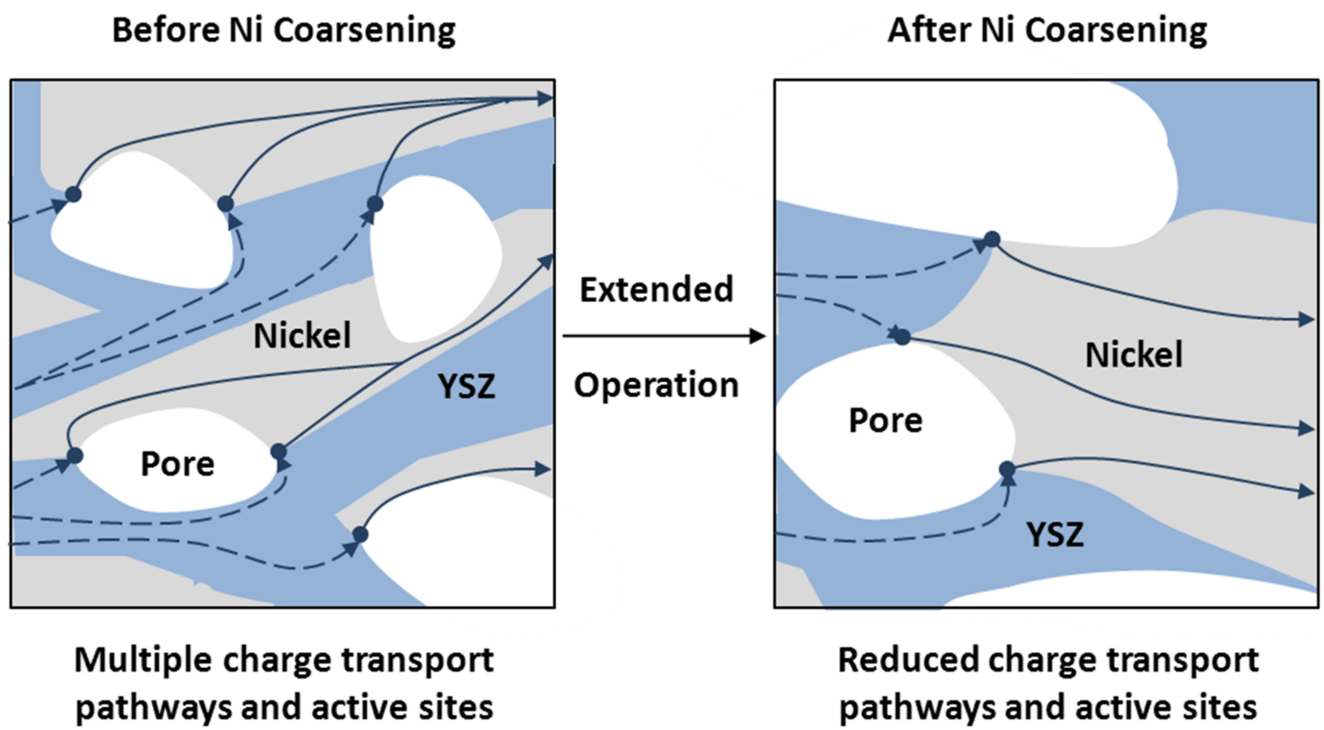

Dihedral Angle Measurement

- Iterative search of RVE identifies two-phase and three-phase boundaries.
- Spline interpolation between voxels determines local dihedral angle.
- A distribution of dihedral angles is calculated based on the local angles.

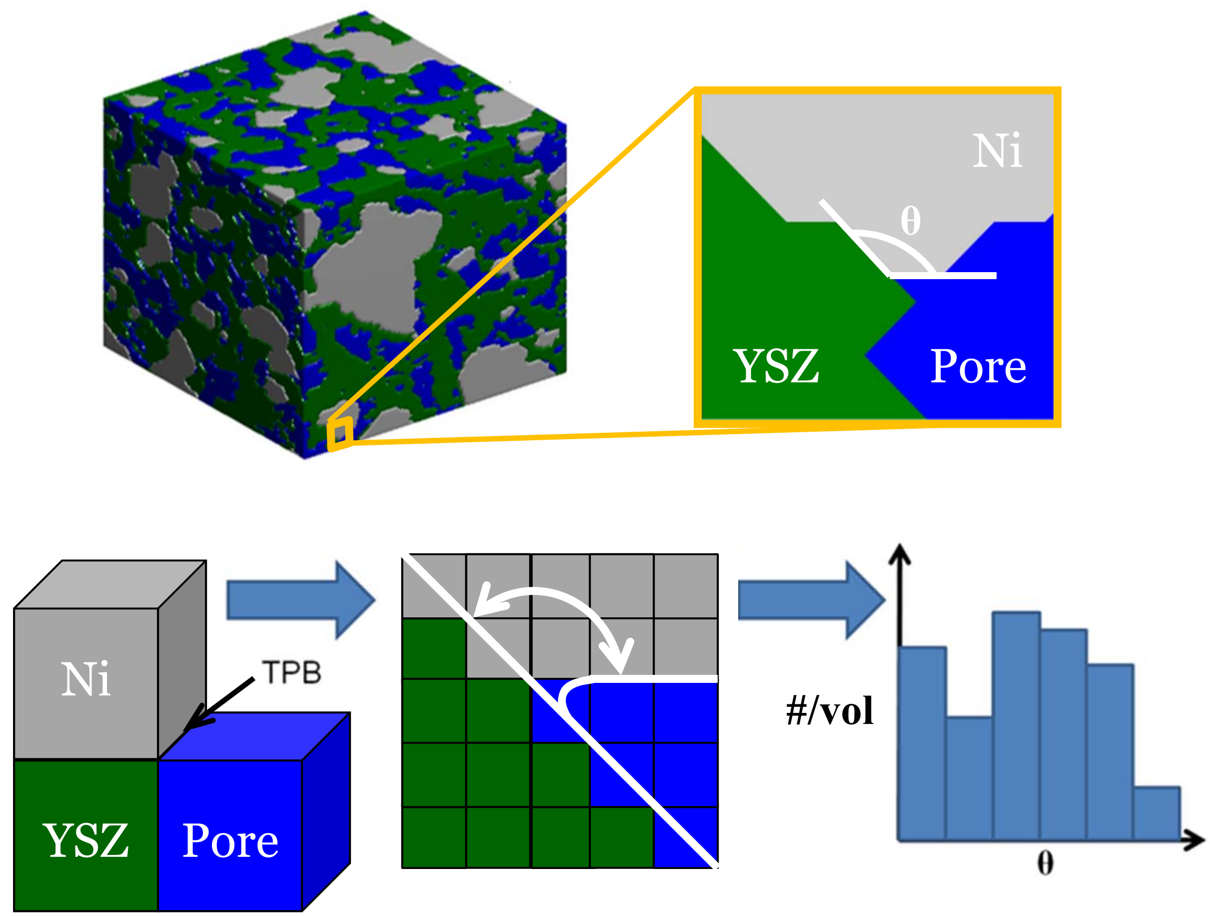

G. J. Nelson, W. K. S. Chiu et al., Acta Materialia, **60** *3491–3500*, 2012.